International Journal of Thermophysics, Vol. 25, No. 1, January 2004 (© 2004)

A Rational Fundamental Equation of State for Pentafluoroethane with Theoretical and Experimental Bases

I M. Astina[1] **and H. Sato**[1,2]

Received July 21, 2003

A fundamental equation of state for pentafluoroethane was established on the basis of not only assessment of the experimental data but also by introducing parameters for virial coefficients having a theoretical background in statistical thermodynamics. The equation of state has a range of validity for temperatures from the triple point up to 500 K and pressures up to 70 MPa. The estimated uncertainties of the equation are 0.1% for the vapor pressure, 0.15% in density for the saturated-liquid phase, 0.5% in density for the saturated-vapor phase, 0.1% in density for the liquid phase, 0.1% in pressure for the gaseous phase, 0.5% in density for the supercritical region, 0.01% in speed of sound for the gaseous phase, 0.9% in speed of sound for the liquid phase, 0.5% in isobaric specific heat for the liquid phase, and 1.2% in isochoric specific heat for the liquid phase. The derived specific heats in the gaseous phase are close to the values from the virial equation of state with the second and third virial coefficients derived from intermolecular potential models and precise speed-of-sound measurements.

KEY WORDS: equation of state; intermolecular potential model; HFC refrigerants; R125; thermodynamic properties.

1. INTRODUCTION

Pentafluoroethane (HFC-125 or R125) is an alternative refrigerant proposed as a component of hydrofluorocarbon (HFC) mixtures such as

[1] Center for Space and Environmental Design, School of Science for Open and Environmental Systems, Graduate School of Science and Technology, Keio University, 3-14-1 Hiyoshi, Kohoku-ku, Yokohama 223-8522, Japan.

[2] To whom correspondence should be addressed. E-mail: hsato@sd.keio.ac.jp

0195-928X/04/0100-0113/0

R410A (R32/125) or R407C (R32/125/134a) to replace R22 (cholorodifluoromethane). A fundamental equation of state for a pure fluid has important roles for both pure fluid and mixture applications. Several existing equations for R125 have been proposed such as the MBWR type [1, 2] or the Helmholtz energy type [3–5]. The International Energy Agency (IEA) has chosen the MBWR-type equation of Piao and Noguchi [1] as an International Standard Equation of State. All the equations were developed on the basis of experimental data whose availability was limited in the gaseous phase, especially at low temperatures for both PVT and caloric properties.

Narukawa et al. [6] pointed out that significant differences exist among the equations of state, including the International Standard ones, concerning the derived specific heat values in the gaseous phase for most HFC refrigerants. Inconsistencies in the third virial coefficients were also confirmed in the study. A more comprehensive investigation for the equations of state for all the HFC refrigerants will be discussed in another paper. Concerning these remaining problems, this paper deals with the development of a fundamental equation of state for R125 with a theoretical background including the second and third virial coefficients that were based on an intermolecular potential model deduced by Kojima and Sato [7]. This work is the second in a series for developing fundamental equations of state for new refrigerants including HFC refrigerants. The first report of this series was concerned with the fundamental equation of state for R32 [8].

2. DEVELOPMENT OF FUNDAMENTAL EQUATIONS OF STATE

The development was based on theoretical and empirical aspects for the thermodynamic properties of fluids. Measurable thermodynamic properties are not always adequate as input data for the development of equations of state. Relying only on experimental data might produce an inadequate result. Shortages and inconsistencies of experimental data for the thermodynamic properties always remain as problems in the development of equations. Accompanying theoretical contributions are significant for developing reliable equations of state.

Thermodynamic relations among experimental and derived properties including intermolecular potential theory and the ideal-gas law were considered, and representation of the thermodynamic properties within the experimental uncertainties was required as a criterion in the development. Assessment and involvement of the theoretical background were necessary to judge whether calculated property values are adequate and reliable in the case of those states that cannot be compared with limited experimental

Table I. Relations of Thermodynamic Properties

Property	Relations
Compressibility factor	$Z = 1 + \delta\alpha_\delta^r$
Fugacity	$f(\delta, \tau) = p \exp\{\alpha^r + \delta\alpha_\delta^r - \ln(1 + \delta\alpha_\delta^r)\}$
Isobaric specific heat	$c_p(\delta, \tau)/R = c_v(\delta, \tau)/R + \dfrac{(1 + \delta\alpha_\delta^r - \delta\tau\alpha_{\delta\tau}^r)^2}{(1 + 2\delta\alpha_\delta^r + \delta^2\alpha_{\delta\delta}^r)}$
Isochoric specific heat	$c_v(\delta, \tau)/R = -\tau^2(\alpha_{\tau\tau}^o + \alpha_{\tau\tau}^r)$
Isothermal compressibility	$\kappa(\delta, \tau)\, \rho RT = \{1 + 2\delta\alpha_\delta^r + \delta^2\alpha_{\delta\delta}^r\}^{-1}$
Joule–Thomson coefficient	$\mu(\delta, \tau)\, R\rho = \dfrac{-(\delta\alpha_\delta^r + \delta^2\alpha_{\delta\delta}^r + \delta\tau\alpha_{\delta\tau}^r)}{(1 + \delta\alpha_\delta^r - \delta\tau\alpha_{\delta\tau}^r)^2 + c_v(\delta, \tau)/R(1 + 2\delta\alpha_\delta^r + \delta^2\alpha_{\delta\delta}^r)}$
Pressure	$p(\delta, \tau)/(\rho RT) = 1 + \delta\alpha_\delta^r$
Saturated-liquid specific heat	$c'_s(\delta', \delta, \tau)/R = \dfrac{c_v(\delta', \tau)}{R} + \dfrac{(1 + \delta'\alpha_\delta^{r'} - \delta'\tau\alpha_{\delta\tau}^{r'})}{(1 + 2\delta'\alpha_\delta^{r'} + \delta'^2\alpha_{\delta\delta}^{r'})} \times \left\{ 1 + \delta'\alpha_\delta^{r'} - \delta'\tau\alpha_{\delta\tau}^{r'} - \dfrac{1}{R\rho_c\delta'} \dfrac{dp_s(\delta', \delta, \tau)}{dT} \right\}$
Second virial coefficient	$B(\tau)\, \rho_c = \lim_{\delta \to 0} \alpha_\delta^r$
Specific enthalpy	$h(\delta, \tau)/(RT) = \tau(\alpha_\tau^o + \alpha_\tau^r) + 1 + \delta\alpha_\delta^r$
Specific entropy	$s(\delta, \tau)/R = \tau(\alpha_\tau^o + \alpha_\tau^r) - (\alpha^o + \alpha^r)$
Specific Gibbs free energy	$g(\delta, \tau)/(RT) = 1 + \alpha^o + \alpha^r + \delta\alpha_\delta^r$
Specific internal energy	$u(\delta, \tau)/(RT) = \tau(\alpha_\tau^o + \alpha_\tau^r)$
Specific heat of ideal gas	$c_p^o(\tau)/R = 1 - \tau^2\alpha_{\tau\tau}^o = 1 + c_v^o(\tau)/R$
Speed of sound	$w^2(\delta, \tau)\, M/(RT) = 1 + 2\delta\alpha_\delta^r + \delta^2\alpha_{\delta\delta}^r + \dfrac{(1 + \delta\alpha_\delta^r - \delta\tau\alpha_{\delta\tau}^r)^2}{c_v(\delta, \tau)/R}$
Third virial coefficient	$C(\tau)\, \rho_c^2 = \lim_{\delta \to 0} \alpha_{\delta\delta}^r$
Volume expansivity	$\beta(\delta, \tau)\, T = \dfrac{1 + \delta\alpha_\delta^r - \tau\delta\alpha_{\delta\tau}^r}{1 + 2\delta\alpha_\delta^r + \delta^2\alpha_{\delta\delta}^r}$

Abbreviations:

$$\alpha_\delta = \left(\frac{\partial\alpha}{\partial\delta}\right)_\tau,\ \alpha_\tau = \left(\frac{\partial\alpha}{\partial\tau}\right)_\delta,\ \alpha_{\delta\delta} = \left(\frac{\partial^2\alpha}{\partial\delta^2}\right)_\tau,\ \alpha_{\tau\tau} = \left(\frac{\partial^2\alpha}{\partial\tau^2}\right)_\delta,\ \alpha_{\delta\tau} = \left(\frac{\partial^2\alpha}{\partial\delta\partial\tau}\right),\ \delta = \frac{\rho}{\rho_c},\ \tau = \frac{T_c}{T}$$

data. Since virial coefficients cannot be measured directly, data derived from experimental data should be assessed from a theoretical viewpoint. The intermolecular potential theory viewpoint was thoroughly considered. Reasonable consideration for involving virial coefficients was introduced in our previous paper for R32 [8].

Input data for modeling cover PVT properties in the single phases and saturation phase, specific heats and speed of sound in the single phases, and the second and third virial coefficients. They consist of experimental data and derived data. Experimental data are used as base data. The derived data were calculated from simple correlations for the gaseous phase and saturation to complement the experimental data. Three ancillary equations were used to reproduce the saturation properties from the triple point up to the critical point, as explained in Section 3. The square-well or Stockmayer potential models were considered for representing the second and third virial coefficients, and specific heats in the gaseous phase were derived from an accurate virial equation of state developed by Kojima and Sato [7] on the basis of their speed-of-sound measurements with the ideal-gas specific heat equation developed in this study.

The distribution of the selected experimental data is shown in Fig. 1. PVT data in the superheated-vapor phase consisted of 54 data points of Zhang et al. [10] at temperatures higher than the critical point, 72 points of Boyes and Weber [11], 385 points of de Vries [12], and 63 points of Matsuda et al. [13]. PVT data in the liquid phase consisted of 77 points of Magee [14], 274 points of de Vries [12], 20 points of Defibaugh and Morrison [15], 152 points of Duarte-Garza et al. [16], and 20 points of Matsuda et al. [13]. PVT data in the supercritical phase consisted of 305 points of de Vries [12], 34 points of Duarte-Garza et al. [16], and 31 points of Defibaugh and Morrison [15].

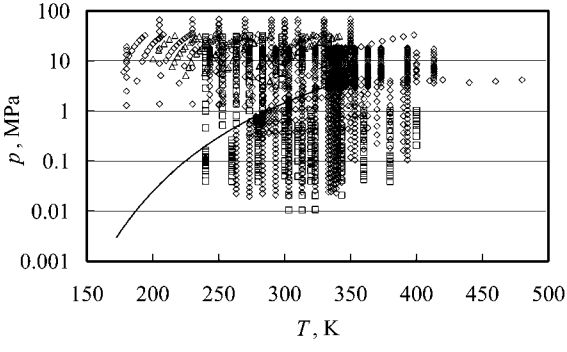

Fig. 1. Selected experimental data for developing the new equation of state. (◇) PVT; (□) w; (△) c_v.

The specific heat data of Lüddecke and Magee [17] were used, consisting of 97 points for the isochoric specific heat in the liquid phase and 93 points for the derived data of the saturated-liquid specific heat. Speed-of-sound data in the gaseous phase consist of 149 points of Gillis [18], 55 points of Kojima and Sato [7], and 69 points of Grigiante et al. [19]. Additionally, 167 points for the speed of sound in the liquid phase by Takagi [20] were used as input data.

3. PARAMETERS AND ANCILLARY EQUATIONS

Several constants for the critical parameters, triple point, molar mass, and gas constant as well as ancillary equations are needed for the development and implementation of the fundamental equation of state. The critical parameters used are the critical temperature of 339.165 K [21] and the critical density of 568 $kg \cdot m^{-3}$ [21]. The critical pressure of 3.6175 MPa was obtained as an extrapolation result of the vapor-pressure equation in this study. Other parameters are the triple-point temperature of 172.52 K [17], the universal gas constant of 8.314472 $J \cdot mol^{-1} \cdot K^{-1}$ [22], and the molar mass of 0.120022 $kg \cdot mol^{-1}$.

Three ancillary equations for calculating vapor pressure, saturated-vapor density, and saturated-liquid density for specified temperatures were developed. The vapor-pressure equation is written as

$$\ln \frac{p_s}{p_c} = \frac{T_c}{T} \sum_{i=1}^{4} N_i \left(1 - \frac{T}{T_c}\right)^{t_i}$$

where $N_1 = -7.532934$, $t_1 = 1$, $N_2 = 1.834267$, $t_2 = 1.5$, $N_3 = -2.852399$, $t_3 = 2.5$, $N_4 = -2.046637$, and $t_4 = 5$. The saturated-liquid density equation is given as

$$\frac{\rho'}{\rho_c} - 1 = \sum_{i=1}^{4} N_i \left(1 - \frac{T}{T_c}\right)^{t_i}$$

where $c_1 = 1.830735$, $t_1 = 1/3$, $c_2 = 0.777434$, $t_2 = 2/3$, $c_3 = 6.326761$, $t_3 = 13/3$, $c_4 = -6.639433$, and $t_4 = 14/3$. The saturated-vapor density equation is expressed as

$$\ln \frac{\rho''}{\rho_c} = \sum_{i=1}^{5} N_i \left(1 - \frac{T}{T_c}\right)^{t_i}$$

where $N_1 = -1.966809$, $t_1 = 1/3$, $N_2 = -9.466522$, $t_2 = 1$, $N_3 = 6.888984$, $t_3 = 4/3$, $N_4 = -17.805099$, $t_4 = 7/3$, $N_5 = -57.623197$, and $t_5 = 6$.

4. NEW FUNDAMENTAL EQUATION OF STATE

The new fundamental equation of state was developed as a functional form of the reduced Helmholtz free energy, which is divided into an ideal-gas part and a residual part. An optimization procedure for selecting the terms of the equation was explained in another paper [23]. The equation of state was developed with a reference point at the saturated liquid of 273.15 K with a specific enthalpy of 200 $kJ \cdot kg^{-1}$ and a specific entropy of 1 $kJ \cdot kg^{-1} \cdot K^{-1}$.

The ideal-gas equation of state is written as

$$\alpha^{\circ} = \ln \delta + \sum_{i=0}^{2} N_i^{\circ} \tau^{b_i^{\circ}} + N_3^{\circ} \ln \tau + \sum_{i=4}^{5} N_i^{\circ} \ln\{1 - \exp(-b_i^{\circ} \tau)\}$$

where $N_0^{\circ} = 13.79478971$, $b_1^{\circ} = 0$, $N_1^{\circ} = 9.231669075$, $b_1^{\circ} = 1$, $N_2^{\circ} = -27.87317349$, $b_2^{\circ} = 0.25$, $N_3^{\circ} = 11.990267052$, $N_4^{\circ} = 7.028445731$, $b_4^{\circ} = 4.907126427$, $N_5^{\circ} = 4.586635360$, and $b_5^{\circ} = 2.080818176$. The parameter δ is ρ/ρ_c and the parameter τ is T_c/T. The residual equation of state is expressed as

$$\alpha^{r} = \sum_{i=1}^{8} N_i \delta^{d_i} \tau^{t_i} + \sum_{i=9}^{17} N_i \delta^{d_i} \tau^{t_i} \exp(-\delta^{e_i})$$

where the numerical coefficients and parameters are given in Table II.

Table II. Coefficients and Parameters of the Residual Part

i	d_i	t_i	e_i	N_i
1	1	0.5	0	1.51628822×10^{0}
2	1	0.75	0	$-1.49598050 \times 10^{0}$
3	1	2.25	0	$-1.28939650 \times 10^{0}$
4	2	0.5	0	1.47295195×10^{0}
5	2	0.875	0	$-2.22976436 \times 10^{0}$
6	2	2	0	1.02082011×10^{0}
7	3	3	0	$-9.61695881 \times 10^{-3}$
8	4	0.5	0	$4.14142522 \times 10^{-2}$
9	3	4	1	$1.46217490 \times 10^{-1}$
10	6	2	1	$-6.56486371 \times 10^{-2}$
11	4	3.25	1	$-9.18319727 \times 10^{-2}$
12	2	9.5	2	$-2.90343386 \times 10^{-2}$
13	4	4.5	2	$-1.74343357 \times 10^{-2}$
14	4	10.5	2	$-8.77406498 \times 10^{-4}$
15	3	25	3	$-5.10648362 \times 10^{-3}$
16	5	5	3	$3.52425947 \times 10^{-3}$
17	7	28	3	$4.98022850 \times 10^{-4}$

5. ASSESMENT AND DISCUSSION

Thermodynamic property values derived from the new fundamental equation of state serve as baselines to express deviations of the experimental data and other derived data. The uncertainty of the new equation of state in representing ideal-gas properties is shown from deviations of the ideal-gas isobaric specific heat in Fig. 2. Deviations for the experimental data by Gillis [18] at temperatures from 240 to 380 K from the new equation of state are 0.15%, 0.05% for the theoretical data by Yokozeki et al. [9] at temperatures from 110 to 1000 K, 0.34% for the data of Grigiante et al. [19] at temperatures from 260 to 360 K, and 0.032% for the equation of Sato et al. [24] at temperatures from 180 to 700 K. The new equation of state represents ideal-gas properties better than the other equations reported in Ref. 1–5.

Experimental data for PVT properties at saturation were compared with the new equation of state. Vapor pressures can be reproduced with an uncertainty of 0.1% and saturation temperatures within 20 mK. Larger percentage deviations occur at lower temperatures, although the absolute deviations are still small. Saturated-liquid and saturated-vapor densities can be reproduced within the uncertainties of 0.15% and 0.5%, respectively, for most temperatures except near the critical temperature. Graphical representations for the saturation properties are given in Figs. 3 and 4.

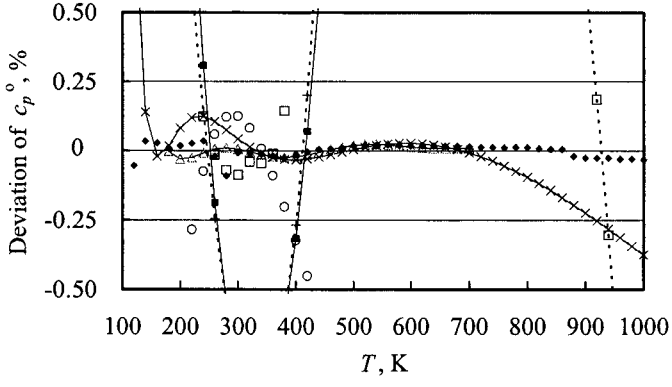

Fig. 2. Deviations of ideal-gas isobaric specific heat from the new equation of state. (□) Gillis [18]; (◆) Yokozeki et al. [9]; (--□--) Vasserman and Fominsky [4]; (○) Grigiante et al. [19]; (–△–) Sato et al. [24]; (–■–) Piao and Noguchi [1]; (--+--) Outcalt and McLinden [2]; (–×–) Sunaga et al. [3].

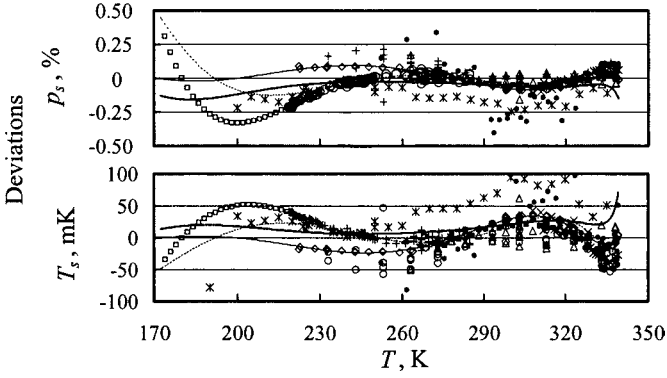

Fig. 3. Deviations of vapor pressure and saturation temperature from the new equation of state. (◇) de Vries [12]; (●) Fukushima [25]; (△) Tsvetkov et al. [26]; (○) Weber and Silva [29]; (+) Oguchi et al. [28]; (∗) Magee [14]; (■) Boyes and Weber [11]; (×) Sagawa [27]; (□) Tillner-Roth [42]; (-----) Piao and Noguchi [1]; (—) Sunaga et al. [3]; (—) Vasserman and Fominsky [4].

Deviations of experimental density, pressure, specific heat, and speed-of-sound data in the single phase are illustrated in Figs. 5 to 9. Figure 5 illustrates the deviations of density measurements in the liquid phase. The deviation is very small at low temperatures, and increases slightly at temperatures close to the critical point. In a range of temperatures below

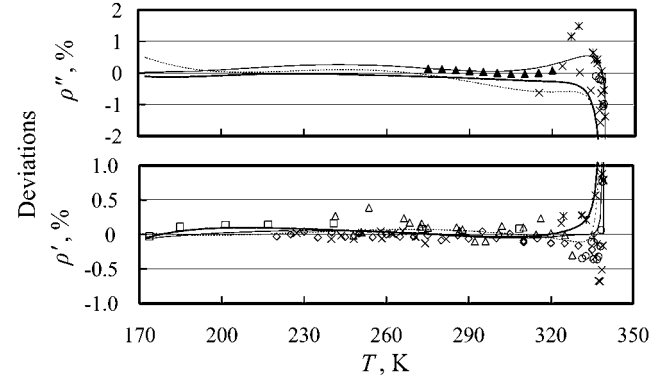

Fig. 4. Deviations of saturated-liquid and saturated-vapor densities from the new equation of state. (×) Fukushima [25]; (○) Kuwabara et al. [21]; (◇) Widiatmo et al. [30]; (□) Magee [14]; (∗) Higashi [31]; (△) Takahashi et al. [32]; (▲) Boyes and Weber [11]; (-----) Piao and Noguchi [1]; (—) Sunaga et al. [3]; (—) Vasserman and Fominsky [4].

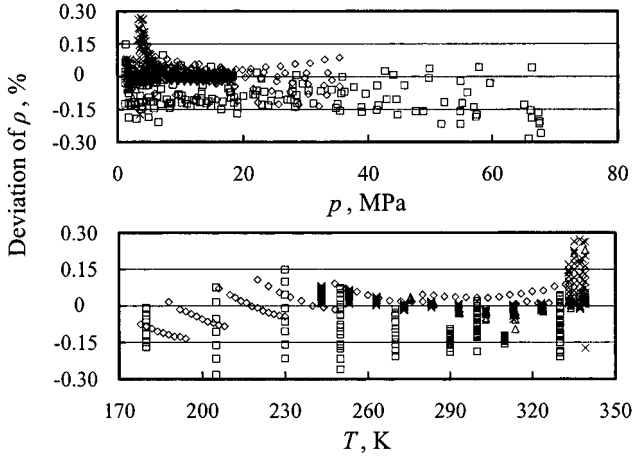

Fig. 5. Deviations of densities in the liquid phase from the new equation of state. (◇) Magee [14]; (×) de Vries [12]; (△) Defibaugh and Morrison [15]; (□) Duarte-Garza et al. [16].

330 K and pressures below 40 MPa, the maximum deviation is 0.15% in density.

The deviations in pressure for numerous sets of experimental data in the gaseous phase from the new equation of state are shown in Fig. 6. The

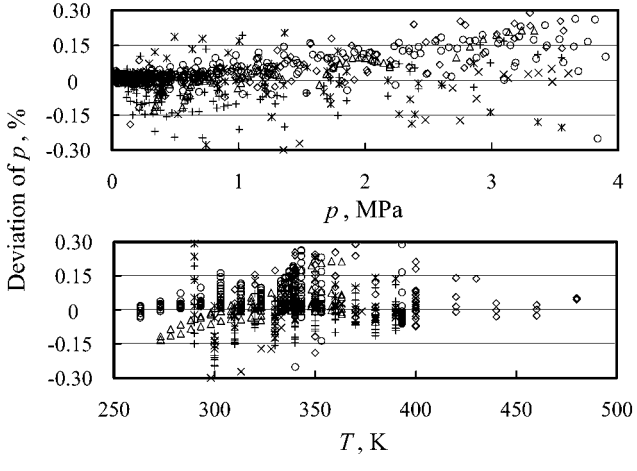

Fig. 6. Deviations of pressures in the gaseous phase from the new equation of state. (◇) Duarte-Garza et al. [16]; (*) Zhang et al. [10]; (+) Ye et al. [33]; (○) de Vries [12]; (△) Boyes and Weber [11]; (□) Duarte-Garza et al. [16]; (×) Oguchi et al. [28].

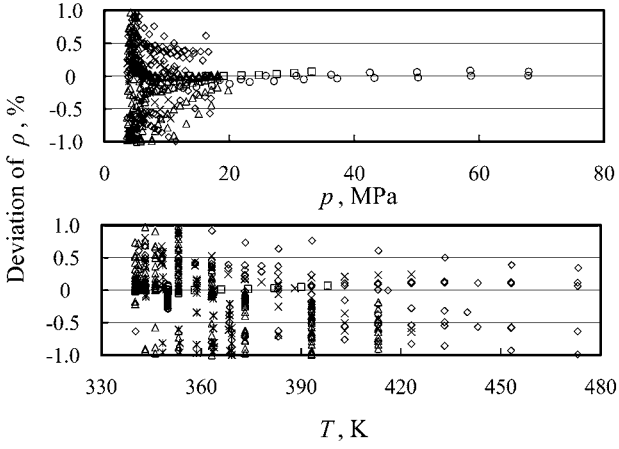

Fig. 7. Deviations of densities in the supercritical region from the new equation of state. (×) Sagawa et al. [27]; (△) de Vries [12]; (∗) Defibaugh and Morrison [15]; (○) Duarte-Garza et al. [16]; (◇) Oguchi et al. [28]; (□) Magee [14].

deviations increase slightly at states near the critical point. The data of de Vries [12] are well represented with an uncertainty of 0.1% at lower pressures and temperatures, while they increase slightly at temperatures near the critical temperature. The data of Duarte-Garza et al. [16] are also reproduced well at higher temperatures.

Figure 7 shows the ability of the new equation of state in representing PVT properties in the supercritical phase. There are slight inaccuracies for the PVT properties in this region as shown for the deviations in the superheated-vapor and liquid phases.

Caloric properties such as the isochoric and isobaric specific heats and the speed of sound are also compared in Figs. 8 and 9. Measurements of Lüddecke and Magee [17] are reproduced mostly within 1.2% as shown in Fig. 8. Although the isobaric specific heats were not fitted in this work, the data of Zhao et al. [34] can be well represented as shown in Fig. 8 within 0.5%. The derived data for the saturated-liquid specific heat by Lüddecke and Magee [17] were used to develop the new equation of state, and those data are represented within 1% of the estimated uncertainties.

Deviations of the speed of sound for both the gaseous and liquid phases are given in Fig. 9. For the speed of sound in the gaseous phase, the new equation of state accurately represents the data of Kojima and Sato [7] with a maximum deviation of 0.02% and an uncertainty of 0.012%; the data of Gillis [18] over a wider range of temperatures and pressures are

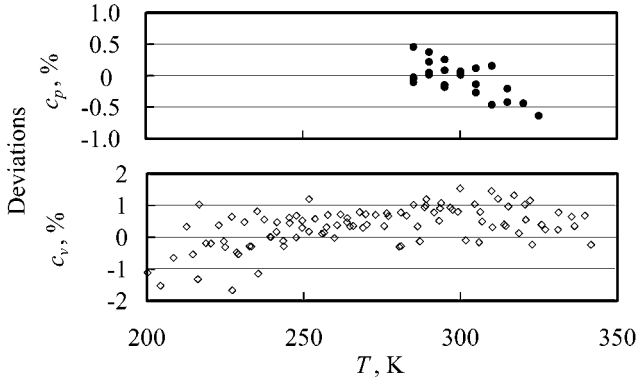

Fig. 8. Deviations of specific heats in the liquid phase from the new equation of state. (◇) Lüddecke and Magee [17]; (●) Zhao et al. [34].

reproduced with a maximum deviation of 0.08% and an uncertainty of 0.044%. On the other hand, the uncertainty for the speed of sound in the liquid phase is larger than that for the gaseous phase, which shows an average uncertainty of 0.8%. More quantitative results for comparisons of experimental data to the values derived from the new equation of state are given in Table III for properties at saturation, and the statistical results for single phases are given in Table IV.

According to the theory of critical phenomenon, the speed of sound should be zero and the isobaric and isochoric specific heats should diverge

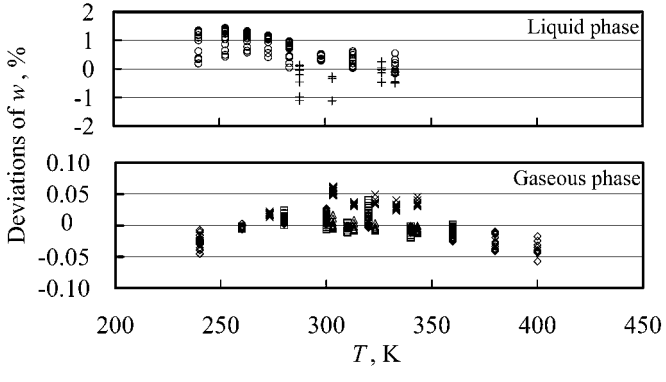

Fig. 9. Deviations of speed of sound from the new equation of state. (◇) Gillis [18]; (×) Hozumi [36]; (△) Kojima and Sato [7]; (□) Grigiante et al. [19]; (+) Grebenkov et al. [35]; (○) Takagi [20].

Table III. Deviations of Measurements at Saturation

First Author	Ref.	N	Prop.	AAD[a] (%)	STD[a] (%)	BIAS[a] (%)	Max. Dev. (%)	N_{out}
Baroncini	38	58	p_s	0.076	0.12	−0.039	0.47	–
Boyes	11	29	p_s	0.031	0.037	−0.016	0.068	–
de Vries	12	104	p_s	0.047	0.055	−0.0095	0.090	–
Duarte-Garza	16	15	p_s	0.11	0.17	0.17	0.71	–
Fukushima	25	45	p_s	0.16	0.19	−0.045	0.57	–
Lüddecke	17	9	p_s	0.12	0.25	−0.0048	0.48	–
Magee	14	33	p_s	0.073	0.14	−0.11	0.58	1
Matsuda	13	22	p_s	0.022	0.028	−0.023	0.059	–
Oguchi	28	61	p_s	0.071	0.10	0.047	0.59	–
Sagawa	27	26	p_s	0.053	0.061	0.0039	0.11	–
Takagi	20	9	p_s	0.25	0.32	0.16	0.73	1
TillnerRoth	42	30	p_s	0.20	0.39	−0.12	1.77	–
Tsvetkov	26	34	p_s	0.037	0.053	0.0018	0.17	–
Weber	29	103	p_s	0.059	0.073	0.040	0.21	–
Widiatmo	30	20	p_s	0.27	0.47	−0.29	1.9	–
Ye	33	12	p_s	0.045	0.053	0.048	0.13	–
Fukushima	25	47	ρ'	0.24	0.41	−0.034	1.1	8
Higashi	31	6	ρ'	0.23	0.36	0.24	0.88	–
Kuwabara	21	9	ρ'	0.25	0.36	−0.13	0.76	–
Magee	14	7	ρ'	0.045	0.063	0.098	0.16	–
Takahashi	32	22	ρ'	0.11	0.14	0.075	0.39	–
Widiatmo	30	25	ρ'	0.050	0.065	−0.049	−0.22	–
Boyes	11	10	ρ''	0.051	0.059	0.049	0.14	–
Fukushima	25	20	ρ''	0.51	0.61	−0.40	1.6	6
Higashi	31	7	ρ''	0.76	0.99	0.27	1.5	–
Kuwabara	21	8	ρ''	0.37	0.44	−0.47	1.1	2
Lüddecke	17	93	c_s'	0.40	0.48	0.11	1.0	–
Kraft	39	13	w'	2.4	2.7	−4.5	7.9	0
Kraft	39	9	w''	1.4	2.1	−0.57	4.0	0

[a] $\mathrm{AAD} = 1/n \sum_{i=1}^{n} |\Delta_i - \mathrm{BIAS}|$; $\mathrm{STD} = \sqrt{1/(n-1) \sum_{i=1}^{n} (\Delta_i - \mathrm{BIAS})^2}$; $\mathrm{BIAS} = 1/n \sum_{i=1}^{n} \Delta_i$; $\Delta = 100(Y - Y_{\mathrm{cal}})/Y_{\mathrm{cal}}$; Y: an evaluated property (Prop.).

infinitely at the critical point. Since experimental data for the caloric properties are not available near and at the critical point, the assessment cannot be conducted for the properties in this region. Therefore, it is not recommended to use the new equation of state for calculating caloric properties in the critical region.

Table IV. Deviations of Measurements in the Single Phase

First Author	Ref.	N	Prop.	Phase[a]	AAD[b] (%)	STD[b] (%)	BIAS[b] (%)	Max. Dev. (%)	N_{out}
Baroncini	38	58	ρ	G	0.38	0.51	−0.20	1.1	–
Boyes	11	80	ρ	G	0.25	0.39	−0.15	1.6	–
Defibaugh	15	232	ρ	L	0.63	0.73	−0.54	2.0	14
de Vries	12	367	ρ	G	0.12	0.23	−0.083	1.9	4
de Vries	12	595	ρ	L	0.35	0.54	−0.11	2.0	14
Duarte-Garza	16	105	ρ	L	0.068	0.085	−0.11	0.29	2
Duarte-Garza	16	213	ρ	G	0.22	0.33	−0.21	1.8	8
Fujimine	40	14	ρ	L	0.023	0.034	−0.0054	0.091	–
Fukushima	37	151	ρ	G	0.69	0.85	−0.42	2.7	9
Magee	14	77	ρ	L	0.044	0.057	0.0021	0.13	–
Matsuda	13	63	ρ	G	0.036	0.043	0.043	0.14	–
Matsuda	13	20	ρ	L	0.017	0.021	0.021	0.043	–
Oguchi	28	167	ρ	G	0.48	0.59	0.25	1.7	–
Sagawa	27	92	ρ	G	0.39	0.54	0.18	2.1	–
Tsvetkov	26	44	ρ	G	0.51	0.61	−0.61	2.3	4
Ye	33	93	ρ	G	0.088	0.13	0.041	0.61	–
Zhang	10	93	ρ	G	0.075	0.12	−0.018	0.64	–
Lüddecke	17	99	c_v	L	0.47	0.62	0.34	1.7	–
Wilson	41	5	c_p	G	1.1	1.7	−0.28	3.1	–
Wilson	41	5	c_p	L	1.0	1.5	0.0018	2.3	–
Zhao	34	24	c_p	L	0.21	0.27	−0.053	0.64	–
Gillis	18	149	w	G	0.014	0.017	−0.0085	0.057	–
Grebenkov	35	29	w	L	0.29	0.38	−0.25	1.1	4
Grigiante	19	69	w	G	0.011	0.014	0.0017	0.040	–
Hozumi	36	72	w	G	0.0081	0.011	0.035	0.062	–
Kojima	7	55	w	G	0.0042	0.0057	−0.0050	0.017	–
Takagi	20	119	w	L	0.40	0.45	0.80	1.4	–

[a] Grouping in accordance with original sources, supercritical phase may be in gaseous (G) or liquid (L) phase.
[b] The same definitions as Table III.

The critical parameters determined from the new equation using the two constraint conditions, i.e., primary and secondary differentiations of pressure with respect to volume at constant temperatures being zero, are 339.165 K for the critical temperature and 568 $kg \cdot m^{-3}$ for the critical density. These values are in accordance with the values selected earlier in this work and with the values recommended by JARef [43]. At these values, the critical pressure calculated from the new equation of state is 3.61746 MPa.

6. FEATURES AND EXTRAPOLATION BEHAVIOR

Consistency of the new equation of state with the intermolecular potential theory was first used in the present study to obtain reliable second and third virial coefficients. Most existing equations of state for R125 (either the Helmholtz energy or MBWR-type functions) can calculate reasonable second virial coefficients in agreement with the intermolecular potential model. On the other hand, the third virial coefficient cannot be uniquely derived as shown from the equations in Fig. 10. The third virial coefficient was difficult to fit using the available experimental data for either the speed of sound or the isobaric specific heat. The third virial coefficients studied by Yokozeki et al. [9] or by Kojima and Sato [7] were carefully assessed and compared with each other. The third virial coefficient of the new equation of state most closely agrees with the calculated results of Yokozeki et al. Yokozeki et al. derived third virial coefficients from the Stockmayer potential model using a theoretical background. On the other hand, Kojima and Sato derived it from their speed-of-sound measurements with an assessment of intermolecular potential models for the square-well and Stockmayer models.

Figure 11 shows comparisons of isochoric specific heats derived from several equations of state for the gaseous phase at low temperatures. The new equation of state can represent the isochoric specific heat close to the values derived from the virial equation of Kojima and Sato [7].

Isochoric and isobaric specific heats and speeds of sound calculated from the new equation of state are shown in Figs. 12 to 14, and isothermal lines of PVT properties are shown in Fig. 15. PVT and caloric properties over a wide range are well represented by the new equation of state.

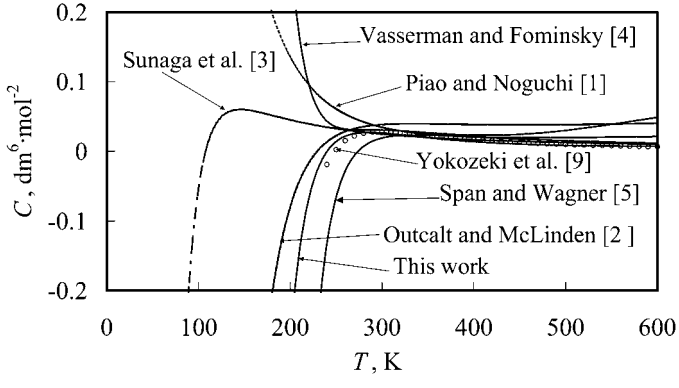

Fig. 10. Comparison of third virial coefficients for several equations of state.

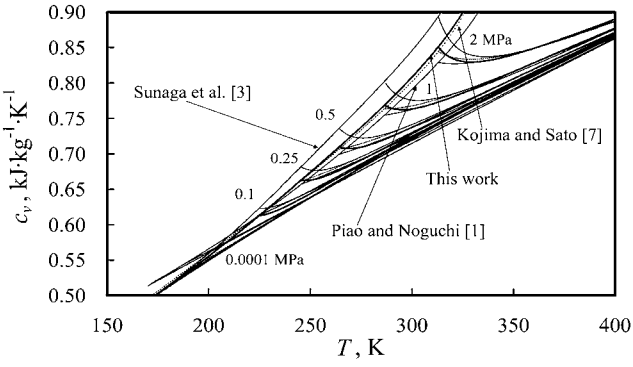

Fig. 11. Comparison of isochoric specific heats in the gaseous phase for several equations of state.

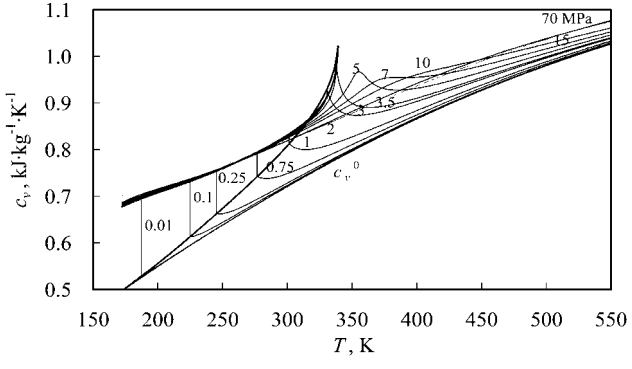

Fig. 12. Isochoric specific heat calculated from the new equation of state.

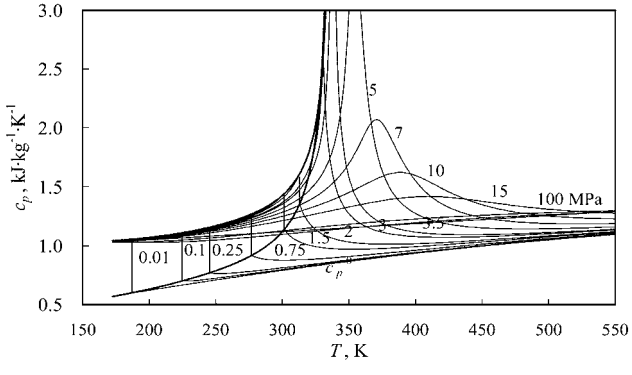

Fig. 13. Isobaric specific heat calculated from the new equation of state.

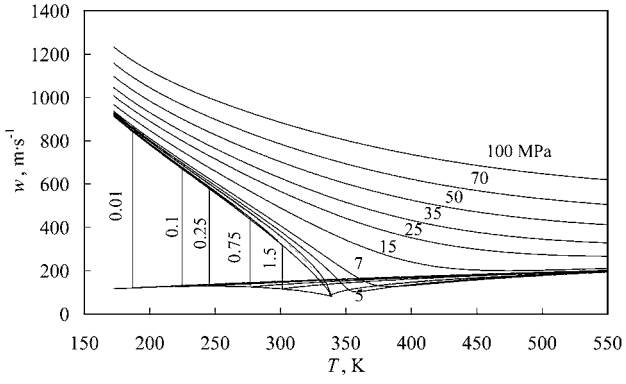

Fig. 14. Speed of sound calculated from the new equation of state.

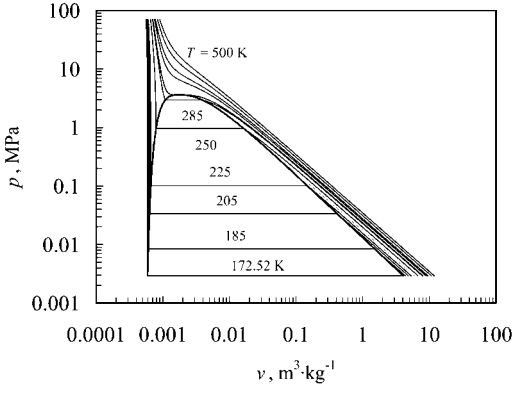

Fig. 15. PVT diagram calculated from the new equation of state.

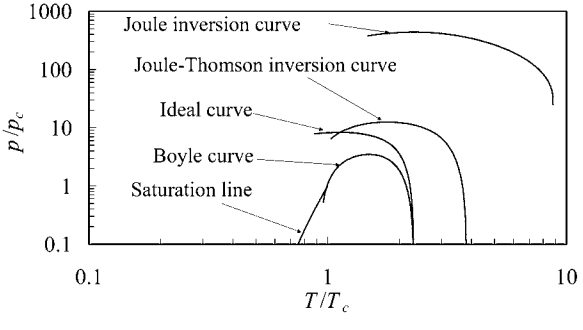

Fig. 16. Characteristic curves of the ideal gas calculated from the new equation of state.

Figure 16 shows reasonable characteristic curves derived from the new equation of state. These reasonable characteristic curves of the ideal gas indicate that the equation of state is acceptable even in the extrapolated range. The new equation of state was examined with experimental data for temperatures up to 480 K and pressures up to 70 MPa. Therefore, the new equation of state is valid for temperatures from the triple point to 500 K and pressures up to 70 MPa.

7. CONCLUSIONS

A fundamental equation of state for R125 was established with rational second and third virial coefficients derived using intermolecular potential theory. The equation of state can provide reliable thermodynamic properties even at very low temperatures and near saturation in the gaseous phase. The specific heat values for the gaseous phase near saturation were reasonably represented without any thermodynamic inconsistency, where large discrepancies are exhibited among existing equations of state.

The new equation of state is effectively applied at temperatures from the triple point to 500 K and pressures up to 70 MPa. The estimated uncertainties of the equation are 0.1% for the vapor pressure, 0.15% in density for the saturated-liquid phase, 0.5% in density for the saturated-vapor phase, 0.1% in density for the liquid phase, 0.1% in pressure for the gaseous phase, 0.5% in density for the supercritical region, 0.01% in speed of sound for the gaseous phase, 0.9% in speed of sound for the liquid phase, 0.5% in isobaric specific heat for the liquid phase, and 1.2% in isochoric specific heat for the liquid phase.

NOMENCLATURE

Notation

a : specific Helmholtz free energy
α : reduced Helmholtz free energy $\alpha = \alpha^{o} + \alpha^{r}$, $\alpha = a/RT$
B : second virial coefficient
β : volume expansivity
C : third virial coefficient
δ : reduced density, ρ/ρ_c
f : fugacity
g : specific Gibbs free energy
h : specific enthalpy
M : molar mass
N : number of data
μ : Joule–Thomson coefficient

κ : isothermal compressibility
p : pressure
R : gas constant, may be in molar or mass unit systems, depending on other property units in the relations
ρ : mass density
s : specific entropy
T : temperature
τ : inverse reduced temperature, T/T_c
u : specific internal energy
v : specific volume
w : speed of sound
Z : compressibility factor

Subscripts

p : process at constant pressure
v : process at constant volume
c : critical parameter
s : saturation

Superscripts

$'$: saturated-liquid state
$''$: saturated-vapor state
r : residual part
o : ideal-gas part
out: rejected

ACKNOWLEDGMENTS

The authors would like to thank Dr. E. W. Lemmon and Dr. D. G. Friend, National Institute of Standards Technology, U.S.A., for valuable suggestions in revising the manuscript.

REFERENCES

1. C. C. Piao and M. Noguchi, *J. Phys. Chem. Ref. Data* **27**:775 (1998).
2. S. L. Outcalt and M. O. McLinden, *Int. J. Thermophys.* **16**:79 (1995).
3. H. Sunaga, R. Tillner-Roth, H. Sato, and K. Watanabe, *Int. J. Thermophys.* **19**:1623 (1998).
4. A. Vasserman and D. V. Fominsky, *Int. J. Thermophys.* **22**:1089 (2001).
5. R. Span and W. Wagner, *Int. J. Thermophys.* **24**:111(2003).
6. K. Narukawa, A. Mizuoka, and H. Sato, presented at *14th Symp. Thermophys. Props.* (Boulder, Colorado, 2000).
7. T. Kojima and H. Sato, *Proc. 16th European Conf. Thermophys. Props. A: Thermophysics of Fluids* (2002).
8. I M. Astina and H. Sato, *Int. J. Thermophys.* **24**:963 (2003).

9. A. Yokozeki, H. Sato, and K. Watanabe, *Int. J. Thermophys.* **19**:89 (1998).
10. H. L. Zhang, H. Sato, and K. Watanabe, *Proc. 19th Int. Cong. Refrig.* (The Hague, 1995), pp. 622–630.
11. S. J. Boyes and L. A. Weber, *J. Chem. Thermodyn.* **27**:163 (1995).
12. B. de Vries, *DKV-Forsch.-Ber. Nr. 55, DKV* (Stuttgart, 1997).
13. N. Matsuda, M. Morishima, and H. Sato, presented at *15th Symp. Thermophys. Props.* (Boulder, Colorado, 2003).
14. J. W. Magee, *Int. J. Thermophys.* **17**:803 (1996).
15. D. R. Defibaugh and G. Morrison, *Fluid Phase Equilib.* **80**:157 (1992).
16. H. A. Duarte-Garza, C. E. Stouffer, K. R. Hall, J. C. Hostle, K. N. Marsh, and B. E. Gammon, *J. Chem. Eng. Data* **42**:745 (1997).
17. T. O. Lüddecke and J. W. Magee, *Int. J. Thermophys.* **17**:823 (1996).
18. K. A. Gillis, *Int. J. Thermophys.* **18**:73 (1997).
19. M. Grigiante, G. Scalabrin, G. Benedetto, R. M. Gavioso, and R. Spagnolo, *Fluid Phase Equilib.* **174**:69 (2000).
20. T. Takagi, *J. Chem. Eng. Data* **41**:1325 (1996).
21. S. Kuwabara, H. Aoyama, H. Sato, and K. Watanabe, *J. Chem. Eng. Data* **40**:112 (1995).
22. J. P. Mohr and B. N. Taylor, *J. Phys. Chem. Ref. Data* **28**:1713 (1999).
23. I M. Astina and H. Sato, presented at *15th Symp. Thermophys. Props.* (Boulder, Colorado, 2003).
24. H. Sato, T. Kojima, and K. Ogawa, *Int. J. Thermophys.* **23**:787 (2002).
25. M. Fukushima, S. Ohotoshi, and T. Miki, *Proc. 19th Int. Cong. Refrig.*, Vol. IVa (1995), pp. 207–214.
26. B. Tsvetkov, A. V. Kletski, Y. A. Laptev, A. J. Asambaev, and I. A. Zausaev, *Int. J. Thermophys.* **16**:1185 (1995).
27. T. Sagawa, H. Sato, and K. Watanabe, *High Temp.-High Press.* **26**:193 (1994).
28. K. Oguchi, A. Murano, K. Omata, and N. Yada, *Int. J. Thermophys.* **17**:55 (1996).
29. L. A. Weber and A. M. Silva, *J. Chem. Eng. Data* **39**:808 (1994).
30. J. W. Widiatmo, H. Sato, and K. Watanabe, *J. Chem. Eng. Data* **39**:304 (1994).
31. Y. Higashi, *Int. J. Refrig.* **17**:524 (1994).
32. K. Takahashi, Y. Takaishi, and K. Oguchi, *Proc. 15th Japan Symp. Thermophys. Props.* (1994), pp. 141–144.
33. F. Ye, H. Sato, and K. Watanabe, *J. Chem. Eng. Data* **40**:148 (1995).
34. X. Zhao, S. Matsueda, and H. Sato, *Proc. 15th European Conf. Thermophys. Props., Comm. B1* (Paderborn, 2001).
35. J. Grebenkov, O. V. Beljajeva, T. A. Zajatz, and B. D. Timofeev, *Proc. 4th Asian Thermophys. Props. Conf.* (Tokyo, 1995), pp. 311–314.
36. T. Hozumi, H. Sato, and K. Watanabe, *Int. J. Thermophys.* **17**:587 (1996).
37. M. Fukushima and S. Ohtoshi, *Proc. 13th Japan Symp. Thermophys. Props.* (1992), pp. 49–52.
38. C. Baroncini, R. Camporese, G. Giuliani, G. Latini, and F. Polonara, *High Temp.-High Press.* **25**:459 (1993).
39. K. Kraft and A. Leipertz, *Int. J. Thermophys.* **15**:387 (1994).
40. L. C. Wilson, W. W. Wilding, G. M. Wilson, R. L. Rowley, V. M. Felix, and T. Chisholm-Carter, *Fluid Phase Equilib.* **80**:167 (1992).
41. T. Fujimine, H. Sato, and K. Watanabe, *Int. J. Thermophys.* **20**:911 (1999).
42. R. Tillner-Roth, *Int. J. Thermophys.* **17**:1365 (1996).
43. JARef, *HFCs and HCFCs*, Version 2.0, JSRAE, Tokyo (in press).